Modeling of Two-Phase Polymerization of Acrylamide in Aqueous Poly(ethylene glycol) Solution

Ting Lü and Guorong Shan
State Key Laboratory of Chemical Engineering, Dept. of Chemical Engineering, Zhejiang University, Hangzhou 310027, China

DOI 10.1002/aic.12459
Published online November 29, 2010 in Wiley Online Library (wileyonlinelibrary.com).

Two-phase polymerization of acrylamide (AM) has been successfully carried out in aqueous poly(ethylene glycol) (PEG) solution with 2,2′-azobis[2-(2-imidazolin-2-yl)propane] dihydrochloride (AIBI) as the initiator. A new heterogeneous kinetic model has been developed based on the partitioning of components between the two phases. It was found that polymerization proceeded in both the continuous and dispersed phases, even though the latter was the dominating polymerization locus. Besides the initiator, monomer concentration, and polymerization temperature, the PEG concentration also significantly influences the polymerization rate. With increasing concentration of PEG, gel effects in the aqueous PAM droplets were enhanced and more monomer preferred to polymerize inside the droplets, hence, the polymerization kinetics accelerated. The proposed model can successfully predict the composition of each phase and the polymerization kinetics during the aqueous two-phase polymerization over a wide range of various reactions conditions. © 2010 American Institute of Chemical Engineers *AIChE J,* 57: 2493–2504, 2011

Keywords: aqueous two-phase polymerization, partitioning, kinetic model, polyacrylamide, poly(ethylene glycol)

Introduction

Polyacrylamide (PAM) is an important synthetic water-soluble polymer that is widely applied in a number of industrial fields, such as wastewater treatment, the oil industry, paper making, and the spinning and printing industries. As a green approach to preparing this water-soluble polymer, the aqueous two-phase polymerization of AM has received great attention in recent years.[1–13] Moreover, the product prepared by aqueous two-phase polymerization can be applied directly in many fields without any separation and redissolution. Therefore, understanding the polymerization mechanism and controlling the polymerization rate during aqueous two-phase polymerization are critical in the production of PAM. Mathematical modeling of the polymerization process is also a key step toward providing opportunities for the optimization of industrial production.

Over the past few decades, many efforts have been devoted to studying the kinetics of aqueous solution polymerization and inverse emulsion (suspension) polymerization of AM. Rodriguez et al.[14] first observed a monomer dependence exceeding first-order in aqueous AM polymerization initiated by potassium persulfate (KPS). This was interpreted in terms of the AM monomer accelerating decomposition of the initiator. Hunkeler et al.[15] proposed a kinetic model that took into account the monomer-enhanced decomposition of KPS, which could accurately predict the aqueous AM polymerization rate. Hamielec et al.[16] established a kinetic model

Correspondence concerning this article should be addressed to G. R. Shan at shangr@zju.edu.cn.

of aqueous AM polymerization at high-monomer concentration by considering diffusion-controlled termination of macroradicals. Regarding the inverse emulsion polymerization of AM initiated by azobisisobutyronitrile (AIBN), Hunkeler et al.[17] studied the polymerization kinetics systematically and established a kinetic model based on the mass transfer of primary radicals between the organic and aqueous phases. When sorbitan monooleate or sorbitan monostearate was used as the emulsifier, the reaction between a macroradical and an interfacial emulsifier dominated over the conventional bimolecular reaction. However, chain transfer to the emulsifier was greatly reduced when using the copolymer polyester-poly(ethylene oxide)-polyester as the emulsifier, thereby resulting in a higher polymerization rate.[18] Xu et al.[19,20] carried out the inverse emulsion polymerization of AM in toluene by using polystyrene-*graft*-polyoxyethylene or poly(methyl methacrylate)-*graft*-polyoxyethylene as the emulsifier. They concluded that the main polymerization location was the aggregated emulsifier molecules around the aqueous droplets, which were swollen by the aqueous monomer solution. In other words, the aqueous droplets merely served as a means of storage of the monomer.

Recently, we studied the droplet formation mechanism of two-phase polymerization of AM in aqueous PEG solution.[21] Primary radicals generated by the decomposition of initiators grow in the continuous phase upon the addition of monomer units until they reach their critical chain length. These macroradicals then precipitate and aggregate, ultimately forming small droplets. Since the monomer and initiator are distributed simultaneously in both the continuous and dispersed phases, the polymerization occurs in both phases, which is quite different from the situation in aqueous solution polymerization or inverse emulsion polymerization. Consequently, it is of significant interest to investigate the partitioning of components between the two phases and the polymerization kinetics of the two-phase polymerization of AM in aqueous PEG solution.

In this research, the effects of polymerization temperature and initial PEG concentration on the partitioning of components between the two phases, as well as the effects of initiator, monomer, and PEG concentrations and temperature on the polymerization kinetics during the aqueous two-phase polymerization have been investigated in detail. Based on the thermodynamic and kinetic characteristics of the aqueous two-phase polymerization, a new mechanistic model is proposed, which has been employed to predict the composition of each phase and the polymerization kinetics during the polymerization of AM in aqueous PEG solution.

Experimental

Materials

Acrylamide (AM, 99.9%, Acros Organics) was of analytical grade and was dried *in vacuo* at 318 K. 2,2′-Azobis[2-(2-imidazolin-2-yl)propane] dihydrochloride (AIBI) as a water-soluble initiator, poly(ethylene glycol) (PEG) with a molecular weight of 20,000 (PEG20000, Acros Organics), and polyacrylamide with a molecular weight of 500,000 (PAM500000, Acros Organics) were used as received without any purification. Deionized water was used throughout this work.

Polymerization procedure

The two-phase polymerization of AM in aqueous PEG solution was performed in a 5×10^{-4} m^3 glass-jacket reactor with a five-necked cover equipped with a motor-driven Teflon stirrer, reflux condenser, argon inlet tube, thermometer, and sampling tube. PEG, AM, and water were added to the reactor, then the mixture was heated to the appointed temperature and purged with argon for 1,800 s. Thereafter, the aqueous initiator solution was injected to start the polymerization. The aqueous two-phase polymerization was carried out under the protection of argon throughout its course. The stirring speed was maintained at 10.5 $rad \cdot s^{-1}$, and the temperature was kept constant.

Characterization methods

Monomer conversions were determined by an improved bromination method as described in our previous article.[21] The sample was treated with hydroquinone once the reactant had been removed. The continuous and dispersed phases were then separated by centrifugation at 1256 $rad \cdot s^{-1}$. The top layer was the continuous phase, while the bottom layer was the dispersed phase. After equilibration at a specified temperature for 86,400 s in a water bath, the volume of each phase could be obtained, and then samples were withdrawn from each layer and their respective AM concentrations were determined by titration (the approach is similar to the monomer conversion measurement). The PEG and PAM mass fractions were determined by a weighing method after drying the samples from each phase *in vacuo* at 323 K. Any remaining AM monomer would have been sublimed under these conditions. The sample obtained from the aqueous two-phase polymerization was directly spread on a microslide, and its microstructure was examined by means of a digital optical phase-contrast microscope (NIKON ECLIPSE E600POL). The viscosity of the polymerization system was determined with an automated viscosity measuring system (HAAKE VT550). The surface tensions of the continuous phase and dilute aqueous PAM solution, as well as the contact angle between the continuous and dispersed phases, were determined by means of a video-based contact angle measuring device (OCA 20). The surface tension of the dispersed phase could be evaluated on the basis of the surface tensions of solid PAM and dilute aqueous PAM solution in conjunction with the PAM content in the dispersed phase. The interfacial tension between the continuous phase and the dispersed phase could then be estimated using the Young equation. UV spectrophotometry (Shimadzu UV-1800) was used to measure the partitioning of AIBI between the two phases, the measurement wavelength for AIBI being 3.595×10^{-7} m. AIBI was introduced into the aqueous two-phase system (PAM500000-PEG20000-H_2O), which was then allowed to equilibrate for 86,400 s at 277 K. The AIBI partition coefficient (the ratio of the AIBI content in the continuous phase to that in the dispersed phase), was then calculated by measuring the AIBI concentration in the continuous phase with respect to the total initial amount of AIBI. To estimate the critical degree of polymerization after which a radical species would precipitate from the continuous phase,

the molecular weight of PAM soluble in the continuous phase was measured. The reaction mixture, equipment, and the procedure at the beginning of the reaction were the same as for the preparation of an aqueous dispersion of PAM. Once phase separation had occurred, hydroquinone (1×10^{-3} kg) was added to stop the polymerization and the PAM droplets were removed by centrifugation. A small portion of the supernatant was dried and the residue was washed with methanol to remove PEG. The dried samples were then diluted with 100 mol·m^{-3} aqueous $NaNO_3$ solution for gel-permeation chromatography (GPC) measurements (Waters 1525 pump, 2414 differential refractometer detector, 717 automatic sample loader). The chromatographic system was made up of three columns connected in series, with stationary phases of PL aquagel-OH 50, 30, and 10, respectively. The mobile phase was 100 mol·m^{-3} aqueous $NaNO_3$ solution, the flow rate was 1.33×10^{-8} m^3·s^{-1}, the sampling volume was 5×10^{-8} m^3, and the column temperature was 303 K.

Model Development

Aqueous two-phase partitioning model

Aqueous two-phase polymerization can be viewed as a special case of precipitation polymerization. During the early polymerization stage, primary radicals formed by the thermal decomposition of initiator molecules rapidly react with monomer molecules to produce polymer chains. Once these macroradicals attain the critical chain length, they separate from the aqueous PEG solution and ultimately aggregate to form PAM droplets. Upon the formation of PAM droplets, polymerization proceeds in two phases, that is, in the continuous phase (PEG-rich phase), and in the dispersed phase (PAM droplets). The dispersed phase contains PAM, monomer, water, and a minor amount of PEG; the continuous phase contains PEG, monomer, water, and a minor amount of soluble PAM. Both the PAM in the continuous phase and the PEG in the dispersed phase will be neglected in our model. It is assumed that, during this polymerization process, the rates of mass transfer of monomer and water from the continuous phase to the dispersed phase are very fast, so that the latter is kept saturated with monomer and water. The treatment of the equilibrium distribution of each component between the two phases is based on the Flory–Huggins theory[22] and the interfacial free-energy theory.[23] At equilibrium, the partial free energy of component i in the continuous phase is equal to that of the same component in the dispersed phase. Applying this to monomer and water leads to Eqs. 1 and 2

$$\begin{aligned}&\ln\phi_{m2}+(1-m_{mw})\phi_{w2}+(1-m_{mp})\phi_{p2}+\chi_{mw}\phi_{w2}^2\\&+\chi_{mp}\phi_{p2}^2+\phi_{w2}\phi_{p2}(\chi_{mw}+\chi_{mp}-\chi_{wp}m_{mw})\\&+2\gamma\overline{V_m}\phi_{p2}^{1/3}/R_0RT-\ln\phi_{m1}-(1-m_{mw})\phi_{w1}\\&-(1-m_{mg})\phi_{g1}-\chi_{mw}\phi_{w1}^2-\chi_{mg}\phi_{g1}^2\\&-\phi_{w1}\phi_{g1}(\chi_{mw}+\chi_{mg}-\chi_{wg}m_{mw})=0\end{aligned}\tag{1}$$

and

Table 1. Solubility Parameters Applied in Eq. 9

Component	Solubility parameter δ_{id} (J·m^{-3})$^{1/2}$	Solubility parameter δ_{ip} (J·m^{-3})$^{1/2}$
AM	15795.6	12092.6
H_2O	15488.8	15998.0
PEG	15343.4	8471.7
PAM	10331.2	11068.0

*Cited from Polymer Handbook and Hansen solubility parameter.[28,29]

$$\begin{aligned}&\ln\phi_{w2}+(1-m_{wm})\phi_{m2}+(1-m_{wp})\phi_{p2}+\chi_{wm}\phi_{m2}^2\\&+\chi_{wp}\phi_{p2}^2+\phi_{m2}\phi_{p2}(\chi_{wm}+\chi_{wp}-\chi_{mp}m_{wm})\\&+2\gamma\overline{V_w}\phi_{p2}^{1/3}/R_0RT-\ln\phi_{w1}-(1-m_{wg})\phi_{g1}\\&-(1-m_{wm})\phi_{m1}-\chi_{wg}\phi_{g1}^2-\chi_{wm}\phi_{m1}^2\\&-\phi_{g1}\phi_{m1}(\chi_{wg}+\chi_{wm}-\chi_{mg}m_{wm})=0\end{aligned}\tag{2}$$

where subscript 1 stands for the continuous phase, 2 for the dispersion phase, m for monomer, w for water, p for PAM, and g for PEG (see also the Appendix), and

$$m_{ij}=\frac{\overline{V_i}}{\overline{V_j}}\tag{3}$$

where $\overline{V}_i$ is the molar volume of component i, and $\overline{V}_J$ is the molar volume of component j. Besides, for the sake of simplicity, the partial molar volume is approximated as the molar volume of the pure component.

Using the material balances of PEG, water, monomer, and PAM, the volume fraction of each component of the system as a function of the volume fraction of water and PAM in the dispersed phase can be obtained (Eqs. 4–7)

$$\phi_{g1}=\phi_{g0}/[1+C\phi_{m0}((\rho_m/\rho_p)\times(1-1/\phi_{p2})-1)]\tag{4}$$

$$\begin{aligned}\phi_{w1}=[\phi_{w0}-\phi_{2w}\phi_{m0}C\rho_m/(\rho_p\varphi_{p2})]/[1+C\phi_{m0}((\rho_m/\rho_p)\\\times(1-1/\phi_{p2})-1)]\end{aligned}\tag{5}$$

$$\phi_{m2}=1-\phi_{w2}-\phi_{p2}\tag{6}$$

$$\phi_{m1}=1-\phi_{w1}-\phi_{g1}\tag{7}$$

Based on the aforementioned theory, the volume and composition of the continuous phase and dispersed phase at every conversion (C) stage during the aqueous two-phase polymerization could be estimated.

The value of the interaction parameter could be calculated using the theory of Hildebrand[24]

$$\chi_{ij}=\overline{V_i}(\delta_i-\delta_j)^2/RT+W_{ij}^s/R\tag{8}$$

where δ is the solubility parameter, and the constant entropic contribution W_{ij}^s/R, generally has a value in the range 0–0.5, where good solubility may be considered as zero.[25] Equation 8 holds well for nonpolar systems and gives a good description of the enthalpic component of the interaction parameter. However, the geometric mean assumption of regular solution theory is not appropriate for polar systems, especially for hydrogen-bonding molecules such as water,[26] and a better model including an extra term describing the interchange

energy density for the solvent—polymer pair was proposed[27,28]

$$\chi_{ij} = \overline{V}_i((\delta_{id} - \delta_{jd})^2 + (\delta_{ip} - \delta_{jp})^2)/RT + W_{ij}^s/R \quad (9)$$

where δ_{id} is the dispersion solubility parameter for component i, and δ_{ip} is the polar solubility parameter for component i. All of the solubility parameters used in Eq. 9 are indicated in Table 1.

Aqueous two-phase polymerization kinetic model

The mechanism of polymerization considered here consists of chemical initiation by first-order decomposition, first-order propagation with respect to the monomer, and chain transfer to produce a dead polymer. In aqueous solution polymerization of AM, macroradicals are disproportionately terminated, hence, second-order termination by disproportionation is taken into account.[15] Chain transfer to water occurred to a negligible extent and no PAM-*g*-PEG was prepared,[21] hence, only chain transfer to the monomer was considered. The reaction scheme can be represented as follows:

Initiation

$$I \xrightarrow{k_d} 2R_0^*$$

$$R_0^* + M \xrightarrow{k_i} R_1^*$$

Propagation

$$R_r^* + M \xrightarrow{k_p} R_{r+1}^*$$

Chain transfer to monomer

$$R_r^* + M \xrightarrow{k_{fm}} P_r + R_1^*$$

Termination

$$R_r^* + R_s^* \xrightarrow{k_{tr}} P_r + P_s$$

After the macroradicals reached their critical chain length (l_{cr}), they precipitated from the continuous phase and ultimately aggregated to form small droplets

$$R_{ie} = k_{p1}[M]_1[R^*_{l_{cr}-1}]_1 \quad (10)$$

The rate of radical absorption onto the aqueous PAM droplets and the rate of radical desorption from the aqueous PAM droplets are needed to calculate the radical concentration, especially that inside the droplets. The aqueous PAM droplets can capture or absorb the radical species in the continuous phase, and the rate of radical absorption (R_{aer}) into the PAM droplets from the continuous phase is expressed by[30]

$$R_{aer} = 4\pi R_0 N D_r / V_1 \quad (11)$$

where R_0 is the mean droplet radius, N is the total number of droplets, D_r is the diffusion coefficient of a radical R_r of which the degree of polymerization is r, and V_1 is the total volume of the continuous phase. The diffusion coefficient D_r can be estimated using the equation proposed by Lusis and Ratcliff.[30]

Nomura et al.[31] derived an expression for the rate coefficient of radical desorption in emulsion polymerization by taking into account the rate of generation of monomeric radicals by chain transfer in polymer particles and the diffusion of these monomeric radicals into the continuous phase. For the dispersion polymerization of styrene in ethanolic media, only the desorption of the monomeric radicals was considered.[32,33] Here, for the sake of simplicity, a coefficient F_{de}, the value of which is between 0 to 1, is introduced to express the radical desorption rate (R_{de}) of both the monomeric and primary radicals

$$R_{de} = F_{de}(k_{fm}[M]_2[R^*]_2 + R_{I2}) \quad (12)$$

Taking into account the capture, desorption, and precipitation of the radicals, as well as the elementary reactions, that is, the initiation reaction of the initiator, the propagation reaction of the growing radicals, the disproportionate termination reaction between two radicals, and chain transfer to the monomer, the balance equations for each growing radical R_r in the continuous phase may be expressed as follows

$$\frac{d[R_1^*]_1}{dt} = R_{I1} - k_{t1}[R^*]_1[R_1^*]_1 - k_{p1}[M]_1[R_1^*]_1 + k_{fm}[M]_1[R^*]_1 + R_{de}V_2/V_1 - R_{ae1} \quad (13)$$

$$\left.\begin{aligned}
\frac{d[R_2^*]_2}{dt} &= k_{p1}[M]_1[R_1^*]_1 - k_{t1}[R^*]_1[R_2^*]_1 \\
&\quad - k_{p1}[M]_1[R_2^*]_1 - k_{fm}[M]_1[R_2^*]_1 - R_{ae2} \\
\frac{d[R_3^*]_3}{dt} &= k_{p1}[M]_1[R_2^*]_1 - k_{t1}[R^*]_1[R_3^*]_1 \\
&\quad - k_{p1}[M]_1[R_3^*]_1 - k_{fm}[M]_1[R_3^*]_1 - R_{ae3} \\
&\cdots\cdots \\
\frac{d[R^*_{l_{rc}-1}]_1}{dt} &= k_{p1}[M]_1[R^*_{l_{cr}-2}]_1 - k_{t1}[R^*]_1[R^*_{l_{cr}-1}]_1 \\
&\quad - k_{p1}[M]_1[R^*_{l_{cr}-1}]_1 - k_{fm}[M]_1[R^*_{l_{cr}-1}]_1 \\
&\quad - R_{ael_{cr}-1}
\end{aligned}\right\} \quad (14)$$

Initiation rate R_I can be expressed as follows

$$R_I = 2fk_d[I_0]\exp(-k_d t) \quad (15)$$

where f is the initiation efficiency, k_d is the initiator decomposition rate constant, k_{p1} is the propagation rate constant in the continuous phase, k_{t1} is the termination rate constant in the continuous phase, I_0 is the initial molar concentration of the initiator, $[M]_1$ is the monomer molar concentration in the continuous phase, and k_{fm} is the rate constant for chain transfer to the monomer. Based on Eqs. 13 and 14, the total radical concentration in the continuous phase can be obtained

$$[R^*]_1 = [R_1^*]_1 + [R_2^*]_1 + [R_3^*]_1 + \cdots\cdots + [R^*_{l_{cr}-1}]_1 \quad (16)$$

When PAM molecules attain a degree of polymerization equal to the critical chain length; they precipitate and form aqueous PAM droplets. Meanwhile, the monomer and initiator can disperse and polymerize in both the continuous and dispersed phases. Taking into account the termination reaction between two radicals, the balance equation for the radical concentration in the dispersed phase may be expressed as follows

Table 2. Summary of Parameters for the Kinetic Model

Parameter	Value	Units	Reference
k_d	1.24×10^{13} exp(-108000/R/T)	s^{-1}	28,35
k_p	1.65×10^{3} exp(-11482/R/T)	$m^3\cdot mol^{-1}\cdot s^{-1}$	18
k_{t1}	1.41×10^{5} exp(-6204/R/T)	$m^3\cdot mol^{-1}\cdot s^{-1}$	18
k_{fm}	9.55×10^{3} exp(-43693/R/T)	$m^3\cdot mol^{-1}\cdot s^{-1}$	18
A	11.22-0.0167T	dimensionless	18
F	[M]/([M]+α)	dimensionless	34
l_{cr}	133	dimensionless	This work

$$\frac{d[R^*]_2}{dt} = R_{I2} + k_{p1}[M]_1[R^*_{l_{cr}-1}]_1 V_1/V_2 - k_{t2}[R^*]_2^2 - R_{de} + \sum_{r=1}^{l_{cr}-1} R_{aer} V_1/V_2 \quad (17)$$

The monomer is consumed by propagation reactions in both the continuous and dispersed phases. The consumption rate of the monomer is given by

$$\frac{dM_t}{dt} = -k_{p1}[R^*]_1[M]_1 V_1 - k_{p2}[R^*]_2[M]_2 V_2 \quad (18)$$

The total molar amount of monomer M_t at time t is related to $[M]_1$, $[M]_2$, V_1, and V_2, the molar concentrations of monomer and the volumes of the continuous and dispersed phases, respectively, by the following mass balance equation

$$M_t = [M]_1 V_1 + [M]_2 V_2 \quad (19)$$

The conversion of monomer is defined by

$$C = (M_0 - M_t)/M_0 \quad (20)$$

Since the viscosity inside the aqueous PAM droplets is high, termination and reaction with terminal double bonds in the dispersed phase will be diffusion-controlled. This has been modeled using the following empirical equations[18]

$$k_{t2} = k_{t1}/\exp(Aw_p) \quad (21)$$

$$A = a - bT \quad (22)$$

where w_p is the mass fraction of PAM in the dispersed phase, A is the gel effective parameter, which is related to the temperature, and a and b are constants.

For the case of aqueous solution polymerization of AM initiated by a water-soluble azo initiator, the initiation efficiency can be expressed as follows[34]

$$f = \frac{[M]}{[M] + \alpha} \quad (23)$$

with $\alpha = 0.97$ at 323 K and 1.20 at 313 K.

The values of each of the kinetic parameters are shown in Table 2.

Model Validation

Composition of each phase during polymerization

In this polymerization systems, the interfacial tension between the continuous phase and dispersed phase was about 1.4×10^{-5} N·m^{-1}, which corresponds to the range reported in standard aqueous two-phase systems.[36,37] Neither the interfacial tension nor the final droplet size had a significant effect on the partitioning of the components between the two phases in the range studied: 0 to 1×10^{-4} N·m^{-1} and 1×10^{-7} to 4×10^{-5} m dia. Similar results have been obtained for the dispersion polymerization of styrene or MMA in aqueous alcoholic media.[25,26]

To test the validity of this model, experiments on the two-phase polymerization of AM in aqueous PEG solution were performed. Figure 1 compares the model predictions of the monomer concentration in each phase at various polymerization temperatures. The model line calculated using the aqueous two-phase partitioning model is in good agreement with the experimental data. With increasing temperature, the

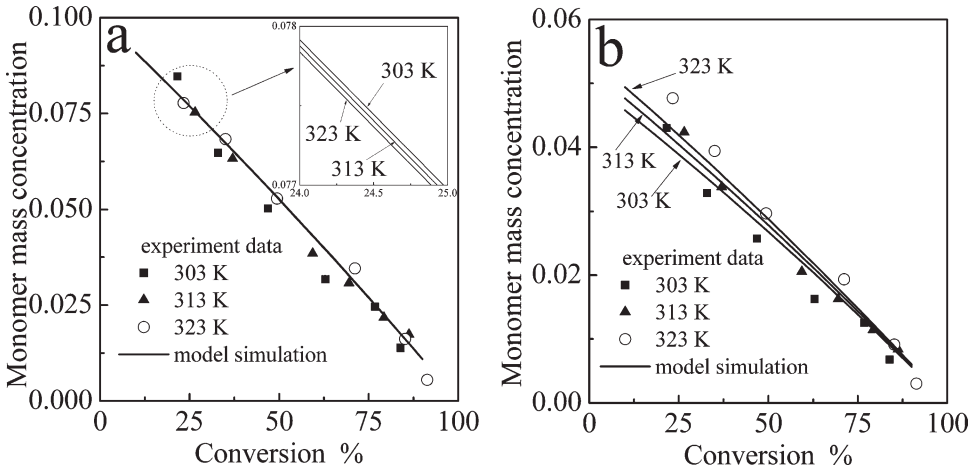

Figure 1. Monomer concentration in each phase during the two-phase polymerization in aqueous PEG solution at various temperatures.

(a) Continuous phase, and (b) dispersed phase (AIBI = 7×10^{-6} kg, AM = 1×10^{-2} kg, PEG = 2×10^{-2} kg, H_2O = 7×10^{-2} kg).

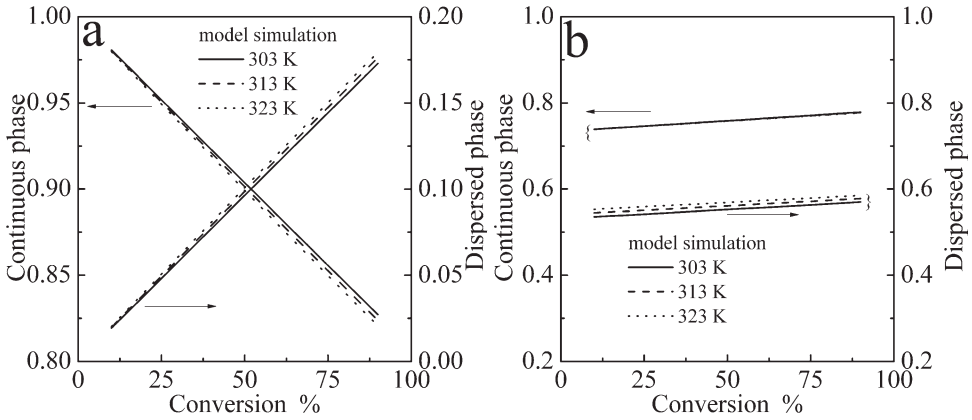

Figure 2. Simulation of the phase volume fraction and water volume fraction of each phase during the two-phase polymerization in aqueous PEG solution at various temperatures.

(a) Phase volume fraction, and (b) water volume fraction in each phase (AIBI = 7×10^{-6} kg, AM = 1×10^{-2} kg, PEG = 2×10^{-2} kg, $H_2O = 7 \times 10^{-2}$ kg).

monomer concentration in the continuous phase decreases very little, while that in the dispersed phase becomes higher. At the beginning of the polymerization, the volume of the dispersed phase is much smaller than that of the continuous phase. As the polymerization proceeds, more and more PAM separates from the continuous phase, while water and the monomer continuously diffuse into the dispersed phase. Thus, the volume of the dispersed phase becomes larger. As shown in Figure 2a, the phase volume fraction of the dispersed phase increases appreciably with increasing polymerization temperature, as well as the monomer concentration in the dispersed phase, which correspond with the slight increase in water content in the dispersed phase shown in Figure 2b. These results indicate that monomer partition is closely related to the water content in each phase. When a solute is distributed in an aqueous two-phase system, its partition coefficient is determined by both entropic and enthalpic contributions.[38] Since the enthalpic contribution in a fixed aqueous two-phase systems will clearly not be changed, we can suppose that it is constant. Therefore, the partition coefficient will be mainly influenced by the entropic contribution, which is usually determined by the number density of molecules. Under such conditions, the solute will migrate to the phase with the highest number density of molecules. In essence, the phase with the higher number density can accommodate the solute in more ways, thereby increasing its partitioning to that phase. Water is the smallest molecule in this aqueous two-phase polymerization system, and, therefore, it is the most obvious factor affecting the molecular number density. As a result, the monomer partition was varied upon changing the water content in each phase. In Figure 2b, the water contents in both phases are seen to increase slightly, which could be attributed to the consumption of monomer as the polymerization proceeds.

Figure 3 compares the model predictions of the monomer concentration in each phase during the polymerization at various PEG concentrations. The simulation line calculated using the aqueous two-phase partitioning model also agrees well with the experimental data. With increasing PEG concentration, the monomer concentration in the continuous

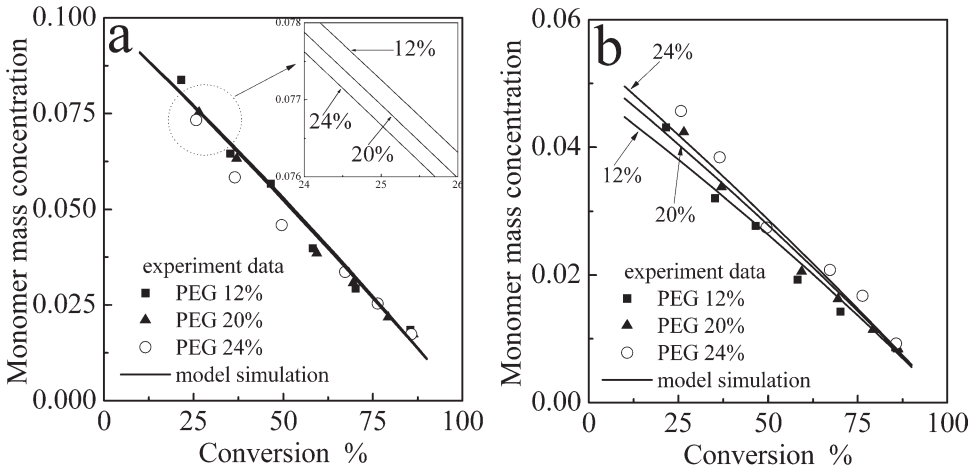

Figure 3. Monomer concentration in each phase during the two-phase polymerization in aqueous PEG solution at various PEG concentrations.

(a) Continuous phase, (b) dispersed phase (AIBI = 7×10^{-6} kg, AM = 1×10^{-2} kg, PEG + H_2O = 9×10^{-2} kg, T = 313 K).

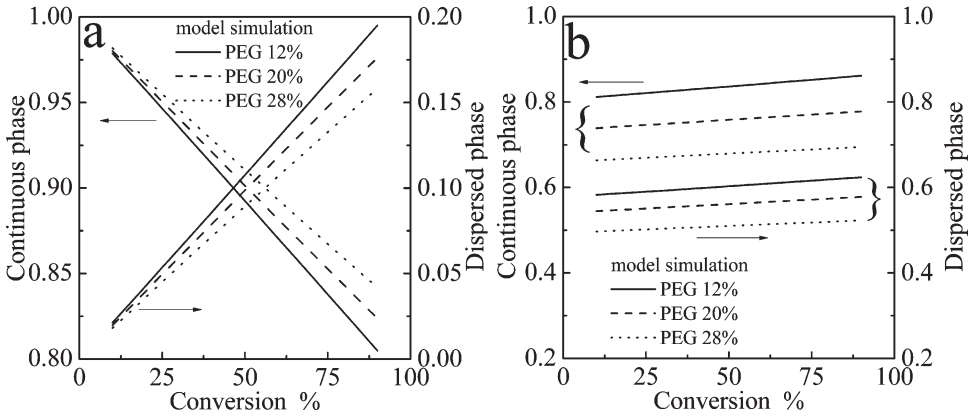

Figure 4. Simulation of the phase volume fraction and water volume fraction of each phase during the two-phase polymerization in aqueous PEG solution at various PEG concentrations.

(a) Phase volume fraction, (b) water volume fraction in each phase (AIBI = 7×10^{-6} kg, AM = 1×10^{-2} k, PEG + H_2O = 9×10^{-2} kg, T = 313 K).

phase decreased slightly, while that in the dispersed phase increased. The volume fraction of the dispersed phase increased with decreasing amount of PEG (Figure 4a), since the dispersed phase could draw more water from the continuous phase. However, it can be seen in Figure 4b that after some of the initial water had been replaced with PEG, the degree of reduction in the water content in the continuous phase was more significant than that in the dispersed phase. Thus, more monomer migrated to the dispersed phase.

The aqueous two-phase partitioning model can predict the monomer concentration in each phase very well for polymerizations with various initial amounts of monomer, as indicated in Figure 5. Besides, Figure 6 shows that this partitioning model also nicely predicts the PEG mass fraction in the continuous phase and the PAM mass fraction in the dispersed phase during the aqueous two-phase polymerization. The small deviations observed in the prediction of PEG mass fraction can be explained in terms of the neglect of the low concentration of PAM that is soluble in the continuous phase. Moreover, Table 3 shows a number of experiments about the PAM mass fraction in the dispersed phase and the PEG mass fraction in the continuous phase in the last stage of the polymerization under various reaction conditions. From Table 3, it seems that the experimental data are in good agreement with the model values. The volume of each phase during the polymerization is also well described by this partitioning model, as shown in Figure 7. All of these results indicate that the proposed partitioning model can quantitatively simulate the composition of each phase during the two-phase polymerization of AM in aqueous PEG solution.

Polymerization kinetics and locus

The initiator partition coefficient was found to vary between 0.6 and 1.3. Figure 8a shows that the partition of the initiator has negligible effect on the polymerization kinetics. This is because the volume of the dispersed phase is much smaller than that of the continuous phase; hence, the partition of the initiator has little influence on the initiator concentration in the continuous phase, especially in the

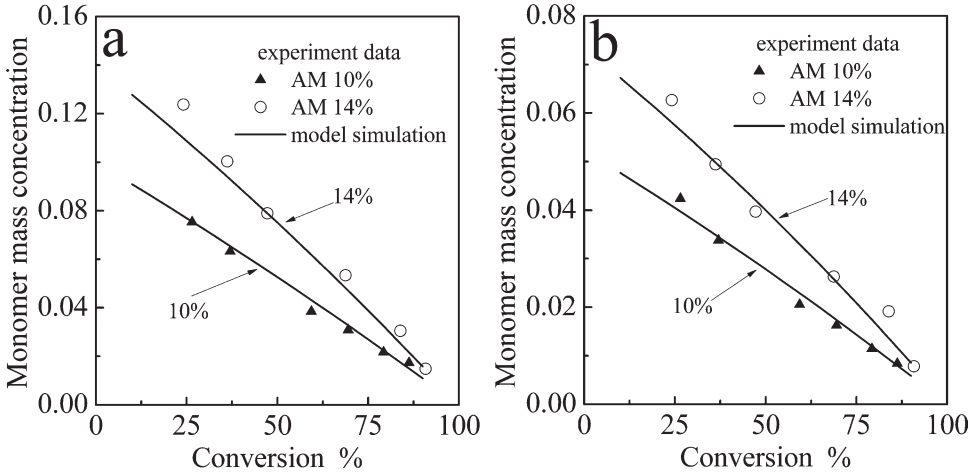

Figure 5. Monomer concentration in each phase during the two-phase polymerization in aqueous PEG solution at various AM concentrations.

(a) Continuous phase, and (b) dispersed phase (AIBI = 7×10^{-6} kg, PEG = 2×10^{-2} kg, AM + H_2O = 8×10^{-2} kg, T = 313 K).

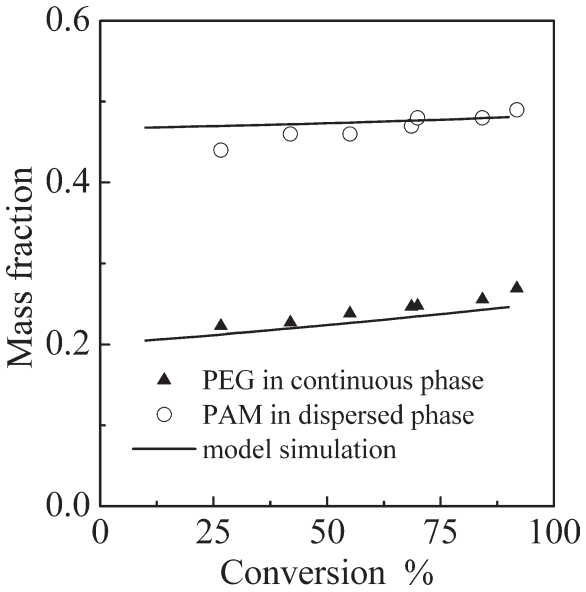

Figure 6. PEG mass fraction in the continuous phase and PAM mass fraction in the dispersed phase during the two-phase polymerization in aqueous PEG solution.

(AIBI = 7×10^{-6} kg, PEG = 2×10^{-2} kg, AM = 1×10^{-2}, $H_2O = 7 \times 10^{-2}$ kg, T = 313 K).

initial polymerization stage. Macroradicals with a degree of polymerization exceeding the critical length would be separated and concentrated in the dispersed phase. As a result, the radicals decomposed from the initiator in the dispersed phase were much fewer compared to those precipitated from the continuous phase. Even though the initiator partition was assumed to be 1000, it can be seen in Figure 8a that the polymerization kinetics did not display any significant difference. This result further confirms that initiator partition in the normal range of this polymerization system has little effect on the polymerization kinetics.

In conventional dispersion polymerization, the polymer particles usually absorb the macroradicals from the continuous phase before they attain the critical chain length. Therefore, almost no new particles are generated after the particle formation stage. In other words, the particle number remains almost constant in conventional dispersion polymerization. Consequently, the radical absorption must be taken into account in the modeling of conventional dispersion polymerization. However, in aqueous two-phase polymerization, small droplets separate from the continuous phase throughout the whole polymerization process. Meanwhile, droplet aggregations is gradually restrained during this polymerization process, hence, polydisperse droplets with both spherical and irregular shapes and of large and small sizes are obtained, as shown in Figure 9. Because of the polydisperse droplets, it is difficult to accurately calculate the absorption of radicals. Here, we use the mean droplet size to estimate the effects of radical absorption on the polymerization kinetics. In the initial stage of polymerization (ca. 5% conversion), the droplet size (mean value about 1×10^{-7} m) was relatively uniform, and nearly all of the droplets were spherical.[21] Based on the aqueous two-phase partitioning model, we can obtain the volume of the dispersed phase at this time, and so the droplet number could be calculated (ca. 1.8×10^{15}). The viscosity of the continuous phase could be regarded as the viscosity of the polymerization system, since the viscosity of the whole system was mainly determined by that of the continuous phase. Assuming the radical absorption rate to be constant throughout the whole process and equal to that at 5% conversion, the influence of radical absorption on the polymerization rate could be evaluated. Actually, the absorption rate will be gradually reduced because of increasing viscosity as the polymerization proceeds. From Figure 8b, it would seem that the radical absorption in this process has little effect on the polymerization kinetics, even though the viscosity (0.05 Pa·s) used in the calculation is lower than the experimental value (0.09 Pa·s). This result gave additional evidence that radical absorption by aqueous PAM droplets present in this polymerization system occurred only to a minor extent, and, therefore, many radicals precipitated to continuously form new small droplets, as described in detail in an early publication.[21]

The effect of radical desorption on the polymerization kinetics is shown in Figure 8c. Even though all of the monomeric and primary radicals were absorbed from the PAM droplets ($F_{de} = 1$), the polymerization kinetics changed very little. This might be attributed to the chain-transfer constant being much smaller than the chain propagation constant (for example, at 313 K, K_{fm} is 4.83×10^{-4} $m^3 \cdot mol^{-1} \cdot s^{-1}$, but k_p is 20 $m^3 \cdot mol^{-1} \cdot s^{-1}$), so that the concentration of monomeric radicals is very low. On the other hand, since, as described earlier, the initiation in the dispersed phase has little effect on the

Table 3. Comparisons Between the Experimental Data and the Model Values for the Two-Phase Polymerization of AM in Aqueous PEG Solution

Run	AM ($\times 10^{-3}$ kg)	PEG ($\times 10^{-3}$ kg)	AIBI ($\times 10^{-6}$ kg)	H_2O ($\times 10^{-3}$ kg)	T (K)	Monomer conversion (%)	PEG mass fraction in the continuous phase (%)		PAM mass fraction in the dispersed phase (%)	
							Exp. data	Model value	Exp. data	Model value
1	6	12	7.0	82	313	89.36	14.27	13.59	38.69	39.71
2	10	20	7.0	70	313	94.54	26.94	25.08	49.08	49.11
3	14	20	7.0	66	313	97.27	30.12	28.15	52.97	51.36
4	10	12	7.0	78	313	93.86	15.32	15.62	41.92	43.36
5	10	16	7.0	74	313	94.65	21.37	20.01	43.87	45.65
6	10	24	7.0	66	313	95.83	30.38	29.24	48.43	50.95
7	16	12	3.5	72	313	97.72	20.27	18.12	42.39	44.70
8	14	16	7.0	70	303	97.19	23.73	21.97	46.28	47.73
9	12	20	3.5	68	323	90.48	26.89	25.96	45.79	48.23

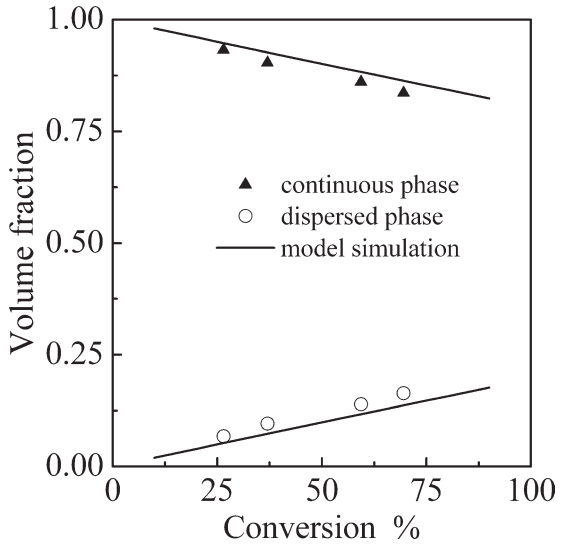

Figure 7. Phase volume fraction of each phase during the two-phase polymerization in aqueous PEG solution.

(AIBI = 7×10^{-6} kg, AM = 1×10^{-2} kg, PEG = 2×10^{-2} kg, $H_2O = 7 \times 10^{-2}$ kg, T = 313 K).

kinetics, desorption of primary radicals in the dispersion can also be ignored. Therefore, radical desorption could be neglected in this aqueous two-phase polymerization system.

The validation of the kinetic model is shown in Figure 10, and the simulation of the contribution of each phase to the conversion is shown in Figure 11. The kinetic model can predict the conversion versus time behavior very well over the range of initiator concentrations studied, as indicated in Figure 10a. With increasing initiator concentration, the initiation points in the continuous phase increased, hence more monomer was consumed in this phase. As in the situation calculated by the kinetic model, it can be seen in Figure 11a that the contribution of the continuous-phase polymerization to the conversion (C_c contribution) increased with increasing initial amount of initiator.

The model predictions of the conversion versus time data at various levels of monomer concentration are also excellent, as indicated in Figure 10b. The contribution of the dispersed-phase polymerization to the conversion (C_d contribution) decreased with decreasing initial amount of monomer, as shown in Figure 11b. This can be explained in terms of the gel effect inside the aqueous PAM droplets. At low-monomer concentration, the PAM fraction of the dispersed phase is lower, resulting in less gel effect at each conversion stage. Therefore, the consumption of the monomer in the dispersed phase slowed and the polymerization ratio inside the droplets decreased.

Figure 10c shows experimental conversion—time data and kinetic model predictions for the two-phase polymerization of AM in aqueous PEG solution at 303, 313 and 323 K, respectively. The kinetic model can be seen to give excellent agreement with the experimental data over all temperatures investigated. This result, together with Eq. 23, suggests that

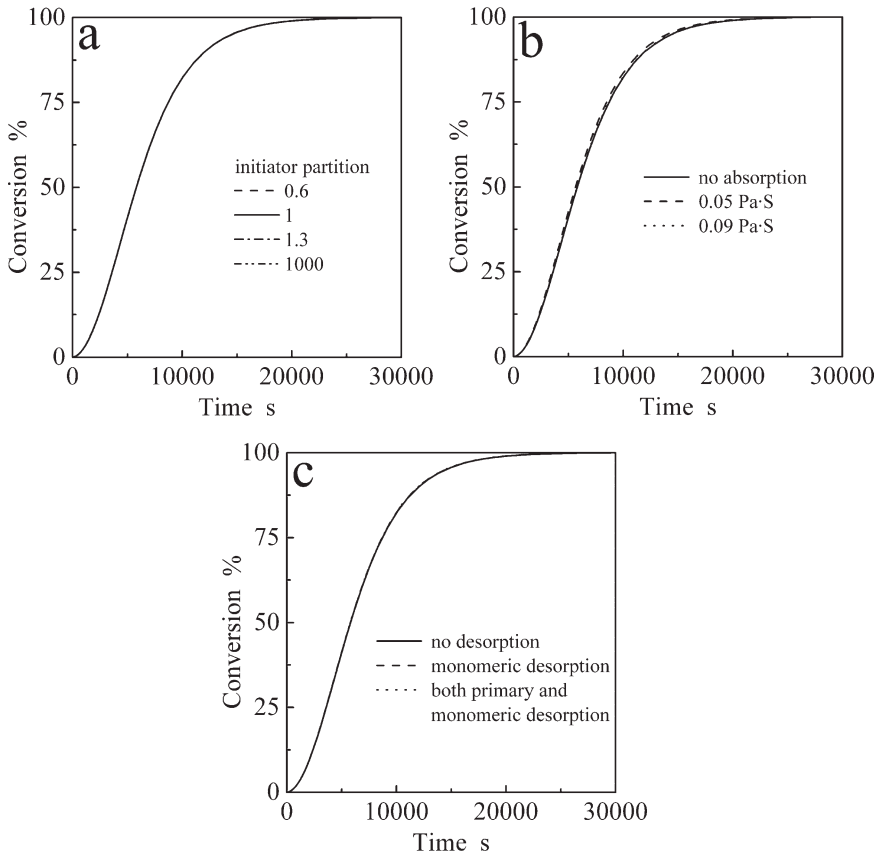

Figure 8. Simulation of the effects of the initiator partition, radical absorption and desorption on the polymerization kinetics during the two-phase polymerization in aqueous PEG solution.

(a) Initiator partition, (b) radical absorption, and (c) radical desorption.

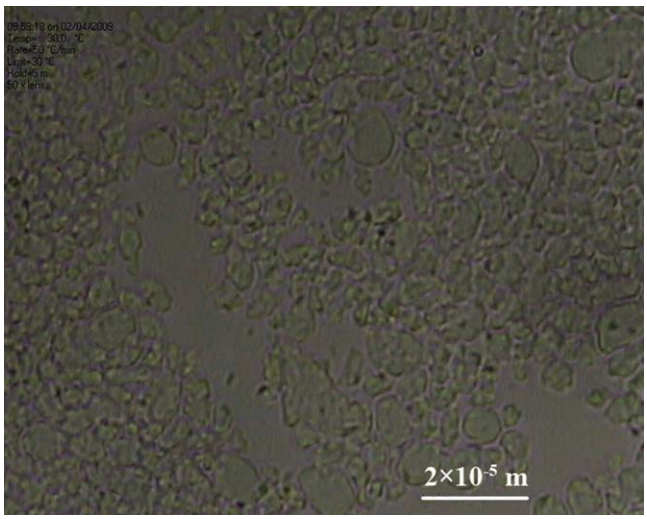

Figure 9. Microstructure of the product prepared through the two-phase polymerization of AM in aqueous PEG solution.

the initiation efficiency of AIBI in the range 303 to 323 K in this polymerization system does not vary significantly. However, in the aqueous solution polymerization of AM initiated by KPS, the initiation efficiency decreased dramatically with increasing temperature. This could be interpreted in terms of the complex-cage theory, which accounts for the monomer-enhanced decomposition of KPS.[15] With increasing temperature, the water content in the dispersed phase increased, and, therefore, the gel effect was suppressed, which would reduce the contribution of the dispersed phase to conversion. However, more monomer is distributed in the dispersed phase and the greater volume of the dispersed phase compensates the former factor. Thus, the contributions of the continuous-phase and dispersed-phase polymerization to the conversion do not change significantly (Figure 11c).

Figure 10d illustrates the effects of PEG concentration on the polymerization rate. The polymerization kinetics accelerated with increasing initial PEG concentration, which corresponds with the model predictions. This validates the rationality of the partitioning model applied to simulate the composition of each phase during the aqueous two-phase polymerization. With increasing initial PEG concentration, the gel effect increased and more monomer was distributed in the dispersed phase, although the volume of the dispersed phase decreased. The former two factors forcing more monomer to polymerize in the dispersed phase exceeded the reverse effect of the latter factor, hence, the polymerization kinetics accelerated and the contribution of the dispersed-

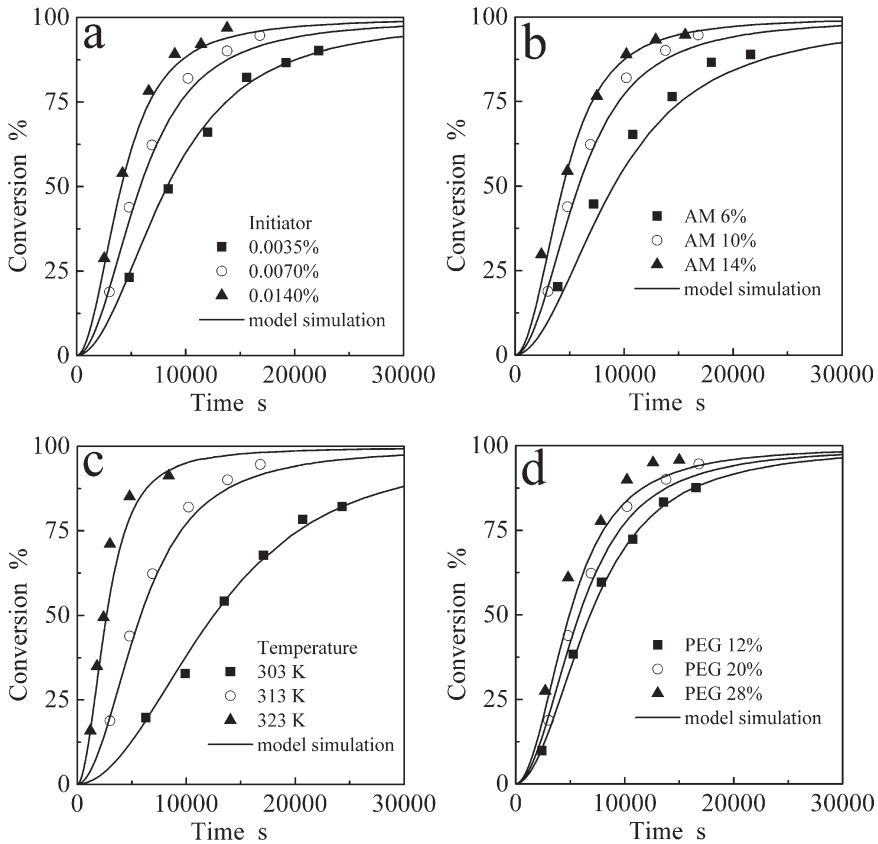

Figure 10. Effect of various polymerization parameters on the polymerization kinetics of the two-phase polymerization in aqueous PEG solution.

(a) initiator concentration (AM = 1×10^{-2} kg, PEG = 2×10^{-2} kg, $H_2O = 7 \times 10^{-2}$ kg, T = 313 K), (b) monomer concentration (AIBI = 7×10^{-6} kg, PEG = 2×10^{-2} kg, AM + $H_2O = 8 \times 10^{-2}$ kg, T = 313 K), (c) polymerization temperature (AIBI = 7×10^{-6} kg, AM = 1×10^{-2} kg, PEG = 2×10^{-2} kg, $H_2O = 7 \times 10^{-2}$ kg), (d) PEG concentration (AIBI = 7×10^{-6} kg, AM = 1×10^{-2} kg, PEG + $H_2O = 9 \times 10^{-2}$ kg, T = 313 K).

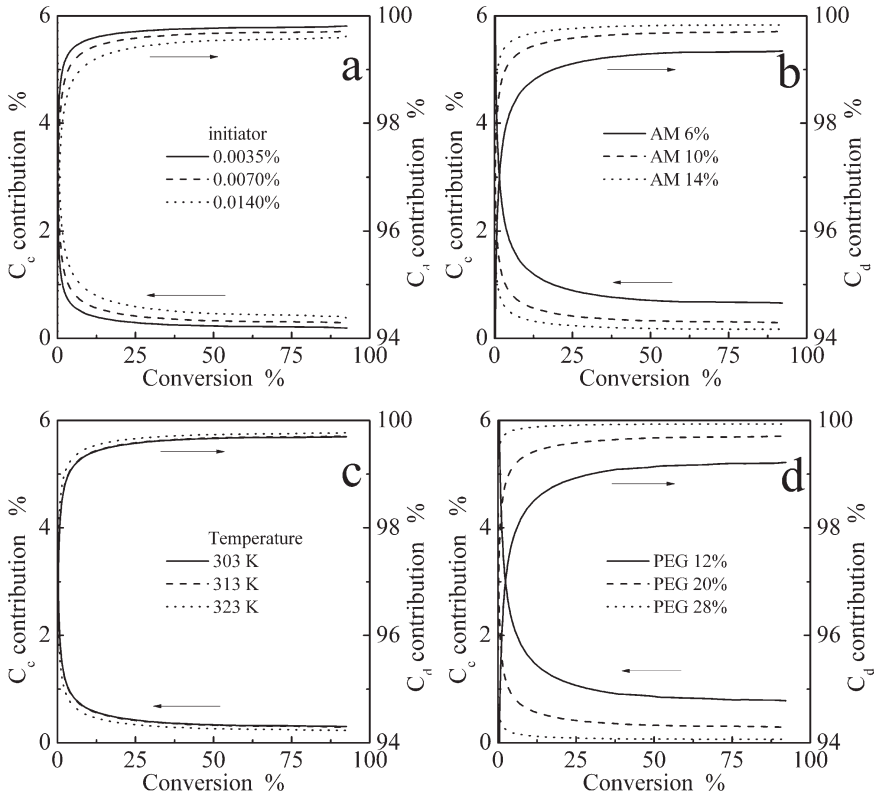

Figure 11. Simulation of the effect of various polymerization parameters on the contribution of each phase to the conversion in the two-phase polymerization in aqueous PEG solution.

(a) Initiator concentration, (b) monomer concentration, (c) polymerization temperature, and (d) PEG concentration.

phase polymerization to the conversion increased, as shown in Figure 11d.

Conclusions

An aqueous two-phase partitioning model has been developed to predict the composition of each phase during the whole polymerization. The predictions of monomer concentration and of PAM and PEG mass fraction in each phase under various polymerization conditions agreed well with the experimental data, indicating that this partitioning model could quantitatively simulate the thermodynamic behavior during the polymerization.

Furthermore, a kinetic model has been proposed for simulating the polymerization kinetics of the aqueous two-phase polymerization of AM in aqueous PEG solution. Calculations based on the kinetic model have shown that the partition of the initiator, radical absorption from the continuous phase, and radical desorption from the dispersed phase have negligible effects on the polymerization kinetics. By systematically investigating the effects of initiator, monomer, and PEG concentration, as well as temperature, on the polymerization kinetics, it was found that the proposed kinetic model can nicely predict the polymerization kinetics over a wide range of polymerization conditions. The contribution of the dispersed-phase polymerization to the conversion increased with increasing initial monomer and PEG concentrations, and with decreasing initiator concentration. However, the polymerization temperature had an insignificant effect on the contribution of each phase to the conversion.

Acknowledgments

The authors thank the financial support from the New Century Excellent Talent Project of Education Ministry (NCET-05-0512), and the National Natural Science Foundation of China (No. 20776125 and 20876136).

Notation

A = gel effect parameter
a = constant
b = constant
C = reaction conversion
D_r = diffusion coefficient of radicals whose degree of polymerization is r, $m^2 \cdot s^{-1}$
F_{de} = coefficient of the radical desorption
f = initiation efficiency of initiator
k_d = decomposition rate constant of initiator, s^{-1}
k_{fm} = chain transfer to monomer constant, $m^3 \cdot mol^{-1} \cdot s^{-1}$
k_i = initiation rate constant, $m^3 \cdot mol^{-1} \cdot s^{-1}$
k_p = propagation rate constant, $m^3 \cdot mol^{-1} \cdot s^{-1}$
k_t = termination rate constant, $m^3 \cdot mol^{-1} \cdot s^{-1}$
l_c = critical chain length
$[M]$ = molar concentration of monomer, $mol \cdot m^{-3}$
M_0 = initial mole of monomer, mol
M_t = total mole of monomer at the reaction time t, mol
m_{ij} = physical constants
R = gas constant, $J \cdot K^{-1} \cdot mol^{-1}$
R_0 = PAM droplet radius, m
R_{aer} = absorption rate of radicals whose degree of polymerization is r, $mol \cdot m^{-3} \cdot s^{-1}$
R_{de} = radical desorption rate, $mol \cdot m^{-3} \cdot s^{-1}$
R_{ie} = precipitation rate of the radicals from the continuous phase, $mol \cdot m^{-3} \cdot s^{-1}$
R_l = initiation rate, $mol \cdot m^{-3} \cdot s^{-1}$
$[R_r^*]$ = molar concentration of radicals whose degree of polymerization is r, $mol \cdot m^{-3}$

r = polymerization degree of the macroradical
T = absolute temperature, K
t = reaction time, s
$\overline{V}i$ = molar volume of component i, m^3
V_i = volume of phase i, m^3

Greek letters

γ = interfacial tension, $N \cdot m^{-1}$
χ_{ij} = interaction parameter of component i and j
ϕ_{ij} = volume fraction of component i in phase j
φi_0 = initial volume fraction of component i
ρ_i = density of component i, $kg \cdot m^{-3}$
δ_i = solubility parameter of component i, $(J \cdot m^{-3})^{1/2}$
δ_{id} = dispersion solubility parameter of component i, $(J \cdot m^{-3})^{1/2}$
δ_{ip} = polar solubility parameter of component i, $(J \cdot m^{-3})^{1/2}$

Subscripts

0 = initial state
1 = continuous phase
2 = dispersed phase
m = monomer
w = water
g = PEG
p = PAM

Literature Cited

1. Song BK, Cho MS, Yoon KJ, Lee DC. Dispersion polymerization of acrylamide with quaternary ammonium cationic comonomer in aqueous solution. *J Appl Polym Sci*. 2003;87:1101–1108.
2. Cho MS, Yoon KJ, Song BK. Dispersion polymerization of acrylamide in aqueous solution of ammonium sulfate: synthesis and characterization. *J Appl Polym Sci*. 2002;83:1397–1405.
3. Liu XG, Chen Q, Xu K, Zhang WD, Wang PX. Preparation of polyacrylamide aqueous dispersions using poly(sodium acrylic acid) as stabilizer. *J Appl Polym Sci*. 2009;113:2693–2701.
4. Chen DN, Liu XG, Yue YM, Zhang WD, Wang PX. Dispersion copolymerization of acrylamide with quaternary ammonium cationic monomer in aqueous salts solution. *Euro Polym J*. 2006;42:1284–1297.
5. Liu XG, Chen DN, Yue YM, Zhang WD, Wang PX. Dispersion copolymerization of acrylamide with acrylic acid in an aqueous solution of ammonium sulfate: synthesis and characterization. *J Appl Polym Sci*. 2006;102:3685–3690.
6. Liu XG, Xiang S, Yue YM, Su XF, Zhang WD, Song CL, Wang PX. Preparation of poly(acrylamide-co-acrylic acid) aqueous latex dispersions using anionic polyelectrolyte as stabilizer. *Colloids Surf A: Physiochem Eng Aspects*. 2007;311:131–139.
7. Wu YM, Wang YP, Yu YQ, Xu J, Chen QF. Dispersion polymerization of acrylamide with 2-acrylamido-2-methyl-1-propane sulfonate in aqueous solution. *J Appl Polym Sci*. 2006;102:2379–2385.
8. Wu YM, Chen QF, Xu J, Bi jM. Aqueous dispersion polymerization of acrylamide with quaternary ammonium cationic comonomer. *J Appl Polym Sci*. 2008;108:134–139.
9. Wu YM, Wang CX, Xu J. Aqueous dispersion polymerization of amphoteric polyacrylamide. *J Appl Polym Sci*. 2010;115:1131–1137.
10. Wang LJ, Wang JP, Yuan SJ, Zhang SJ, Tang Y, Yu HQ. Gamma radiation-induced dispersion polymerization in aqueous salts solution for manufacturing a cationic flocculant. *Chem Eng J*. 2009;149:118–122.
11. Ye Q, Zhang ZC, Ge XW. Highly efficient flocculant synthesized through the dispersion copolymerization of water-soluble monomers induced by γ-ray irradiation: Synthesis and polymerization kinetics. *J Appl Polym Sci*. 2003;89:2108–2115.
12. Li G, Yang C, He YG, Yang F, Yu XQ. Studies of precipitated polymerization of acrylamide with quaternary ammonium cationic comonomer in potassium citrate solution. *J Appl Polym Sci*. 2007;106:2479–2484.
13. He YG, Li G, Yang F, Yu XQ, Cui YJ, Ren FX. Precipitation polymerization of acrylamide with quaternary ammonium cationic monomer in potassium carbonate solution initiated by plasma. *J Appl Polym Sci*. 2007;104:4060–4067.
14. Riggs JP, Rodriguez F. Persulfate-initiated polymerization of acrylamide. *J Polym Sci Part A: Polym Chem*. 1967;5:3151–3165.
15. Hunkeler D. Mechanism and kinetics of the perfulfate-initiated polymerization of acrylamide. *Macromolecules*. 1991;24:2160–2171.
16. Kim CJ, Hamielec AE. Polymerization of acrylamide with diffusion controlled termination. *Polymer*. 1984;25:845–849.
17. Hunkeler D, Hamielec AE, Baade W. Mechanism, kinetics and modelling of the inverse-microsuspension homopolymerization of acrylamide. *Polymer*. 1989;30:127–142.
18. Hernández-Barajas J, Hunkeler DJ. Inverse-emulsion polymerization of acrylamide using block copolymeric surfactants: mechanism, kinetics and modelling. *Polymer*. 1997;38:437–447.
19. Xu ZS, Chen YC, Zhang GJ, Cheng SY, Feng LX. The inverse emulsion polymerization of acrylamide using polystyrene-*graft*-polyoxyethylene as the stabilizer. *J Polym Sci Part A: Polym Chem*. 1999;37:2719–2725.
20. Xu ZS, Yi CF, Cheng SY, Feng LX. The inverse emulsion polymerization of acrylamide using poly(methyl methacrylate)-*graft*-polyoxyethylene as the stabilizer. *J Appl Polym Sci*. 2001;79:528–534.
21. Lü T, Shan GR. Mechanism of the droplet formation and stabilization in the aqueous two-phase polymerization of acrylamide. *J Appl Polym Sci*. 2009;112:2859–2867.
22. Flory PJ. *Principles of Polymer Chemistry*. Ithaca and London: Cornell University Press; 1953.
23. Morton M, Kaizerman S, Altier MW. Swelling of latex particles. *J Colloid Sci*. 1954;9:300–312.
24. Hildebrand JH, Scott RH. *Solubility of Non-Electrolytes*. 3rd ed. New York: Reinhold; 1964.
25. Cao K, Li BG, Pan ZR. Micron-size uniform poly(methyl methacrylate) particles by dispersion polymerization in polar media IV. monomer partition and locus of polymerization. *Colloids Surf A: Physiochem Eng Aspects*. 1999;153:179–187.
26. Lacroix-Desmazes P, Guillot J. Dispersion polymerization of styrene in ethanol-water media: monomer partitioning behavior and locus of polymerization. *J Polym Sci Part B: Polym Phys*. 1998;36: 325–335.
27. Chen SA. Polymer miscibility in organic solvents and in plasticizers-a two dimensional approach. *J Appl Polym Sci*. 1971;15:1247–1266.
28. Brandrup J, Immergut EH, Grulke EA. *Polymer Handbook*. 4th ed. New York: Wiley-Interscience; 1999.
29. Hansen CM. *Hansen Solubility Parameters, A User's Handbook*. 2nd ed. New York: CRC Press; 2007.
30. Yasuda M, Seki H, Yokoyama H, Ogino H, Ishimi K, Ishikawa H. Simulation of a particle formation stage in the dispersion polymerization of styrene. *Macromolecules*. 2001;34:3261–3270.
31. Nomura M, Harada M. Rate coefficient for radical desorption in emulsion polymerization. *J Appl Polym Sci*. 1981;26:17–26.
32. Ahmed SF, Poehlein GW. Kinetics of dispersion polymerization of styrene in ethanol 1. model development. *Ind Eng Chem Res*. 1997; 36:2597–2604.
33. Ahmed SF, Poehlein GW. Kinetics of dispersion polymerization of styrene in ethanol 2. model validation. *Ind Eng Chem Res*. 1997;36:2605–2615.
34. Ishige T, Hamielec AE. Solution polymerization of acrylamide to high conversion. *J Appl Polym Sci*. 1973;17:1479–1506.
35. Fujie H, Shiraki K, Miyagawa T, Minamii N, Yamada B, Otsu T, Preparation and thermal-decomposition of cyclic azoamidinium salts as water-soluble radical initiators for polymerization over a wide temperature-range. *J Macromol Sci Part A: Pure Appl Chem*. 1992;29:741–751.
36. Ryden J, Albertsson PA. Interfacial tension of dextran-polyethylene glycol-water 2-phase systems. *J Colloid Interf Sci*. 1971;37:219–222.
37. Ding P, Wolf B, Frith WJ, Clark AH, Norton IT, Pacek AW. Interfacial tension in phase-separated gelatin/dextran aqueous mixtures. *J Colloid Interf Sci*. 2002;253:367–376.
38. Johansson HO, Karlström G, Tjerneld F, Haynes CA. Driving forces for phase separation and partitioning in aqueous two-phase systems. *J Chromatogr B*. 1998;711:3–17.

Manuscript received May 18, 2010, and revision received Aug. 14, 2010.